**SUPPLEMENTAL MATERIAL for**

**Title:**

Ectopic granule cells in the hilus of the mouse dentate gyrus: effects of age, septotemporal location, strain, and selective deletion of the proapoptotic gene *BAX*.

**Authors:**

Keria Bermudez-Hernandez, Yi-Ling Lu, Jillian Moretto, Swati Jain, John J. LaFrancois, Aine M. Duffy and Helen E. Scharfman

**Contents of Supplemental Material:**

**Supplemental Methods - Quantification of Prox1-ir cells**

With micrographs acquired as described in the Methods section, the hilus was traced in Adobe Photoshop as follows. First the GC layer was traced (A, below) with the magic wand tool and quick selection tool (upper left corner). Then the inverse of the GC layer tracing was outlined in red (B, below) and an area that encompassed the hilus was traced in green. The polygonal lasso tool (upper left corner in B) was used with the “Intersect with selection” command to outline the intersected region (C, below). The selection was contracted by 22 pixels (D, below), which corresponded to 8 μm, the average diameter of a GC, which we determined empirically. This was done to ensure that the hilus did not overlap with a GC in the GC layer that was atypical because it was slightly displaced into the hilus. However, sometimes there was more than one GC that seemed to be displaced into the hilus, and when this occurred the cell was subtracted from the area that was used to define the hilus, and hilar Prox1-ir cells.

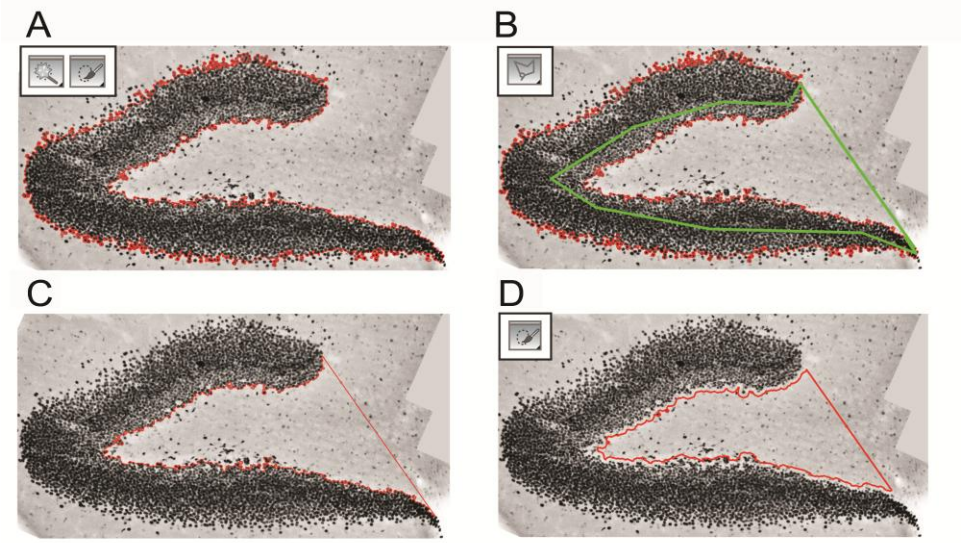


The next step was to use the GC layer to define the average intensity of Prox1-ir of GCs. This was done to set the threshold for defining what level would be used to define a Prox1-ir cell in the hilus, i.e. to differentiate the cells we defined as hilar Prox1-ir cells from lightly stained hilar Prox1-ir cells that we considered to light to be counted. These light cells were similar in their staining intensity to the background staining level. Thus, a cell that was darker than the threshold that was set was counted, and a cell that was lighter was not. Then the

image shown in A, below, was thresholded using the isodata algorithm (Ridler and Calvard, 1978). In other words, it was converted to either white (above threshold) or black (below threshold; shown in B, below). The computer counted only those cells that were above the threshold and had an area > 15 and < 50 $\mu m^2$ (the range of areas of GCs). Note that this area had a large range because some young GCs are small compared to mature GCs and we wanted to count all GCs. The purple box in C (below) is shown in D to illustrate the hilar cells that were selected using the two criteria, threshold and area. They are outlined in red.

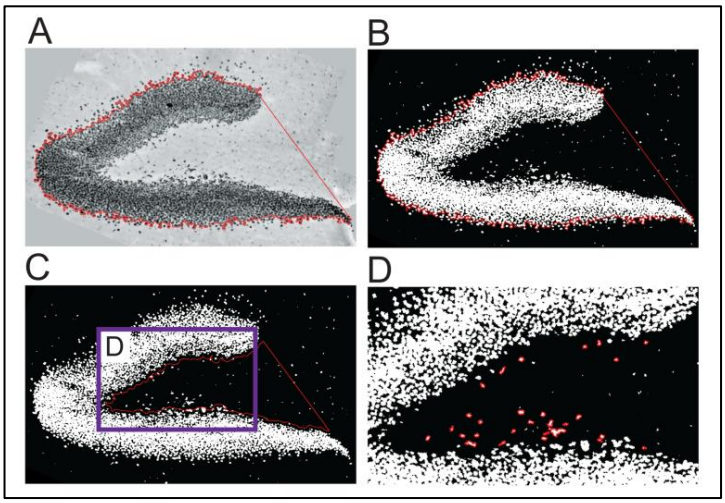


Potential clusters (overlapping cells) were addressed by analyzing the areas that the computer identified were above threshold and larger than 50 $um^2$ in area. In A (below) potential clusters (yellow arrow) are distinguished by single cells (green arrow). To determine the number of cells that corresponded to a potential cluster, the area of the cluster was calculated by the computer and divided by the average area of a single GC (32 $\mu m^2$). In B, a histogram is shown of the results from analysis of 7 sections from 3 mice. When areas that were small (< 50 $\mu m^2$) were examined under the microscope by focusing up and down at high power by eye, they corresponded to a single cell (green bars). When areas that were larger were reviewed by eye, the cluster was typically 1-3 cells (yellow bars). In C, comparisons are made between automated (white bars) and manual (black bars) methods, showing that they were comparable. In D, the means that were computed from the manual and automated method are

compared by a Student's t-test and the differences were not significant (p = 0.338). These comparisons validated the use of automated method for quantification. The comparison in C-D is further informative because it suggests that most of the clusters were composed of average sized- GCs since the value of 32 μm$^2$ led to an accurate analysis.

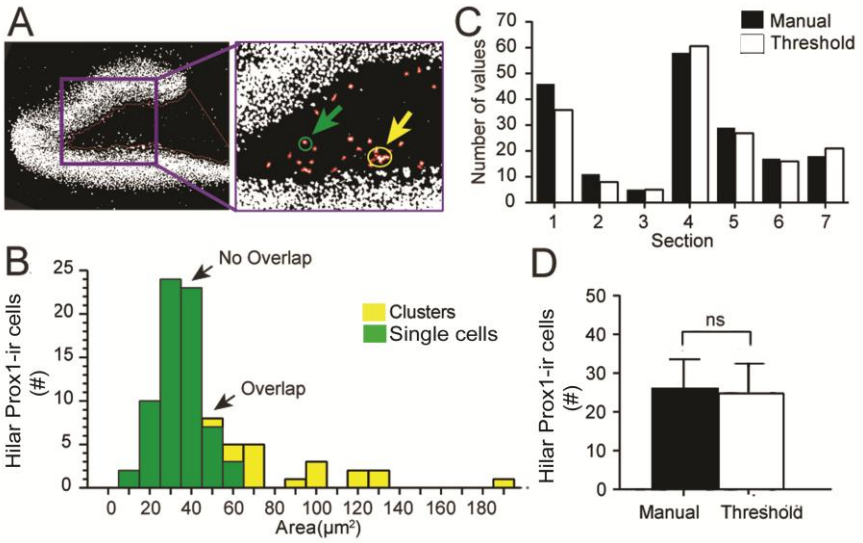


Density was calculated either for a single septotemporal level or the entire hippocampus. To calculate density for a single level, the estimated number of cells of a given section was divided by the area of the hilus in that section. Hilar area was defined by the selected area in part D of the first figure, above.

To estimate the total number of cells per hippocampus, the estimated number of cells for each section was summed. This was only done for analysis of the isolated hippocampus where the entire septotemporal axis was assessed. The total number of cells was divided by the reciprocal of the section sampling fraction (ssf): $N = \frac{1}{ssf} \times \sum n$ . To estimate hilar volume per hippocampus, the following formula was used where T was the section thickness (50 μm) and A the selected hilar area (as shown in the figure, above): $V = \frac{1}{ssf} \times T \times \sum A$.

**Supplemental Table 1. Description of antibodies and their use.**

| Primary antibody | Generation and characterization | Blocking Solution | Secondary antibody |
|---|---|---|---|
| Prox1<br>Brightfield<br><br>Rabbit Polyclonal (AngioBio)<br><br>1:10,000 | Recognizes the C-terminal end of Prox1 and specificity in DG GCs has been demonstrated (Lavado et al., 2010). | 10% goat serum (Vector) in Tris blocking solution* | Goat anti-rabbit (1:400, Vector) |
| Prox1<br>Confocal<br><br>Goat Polyclonal (R&D)<br><br>1:1,000 | Raised against human Prox1. Western blot was used to show that the antibody recognized a 83 kDa protein corresponding to the molecular weight of Prox1 (information from the Manufacturer's datasheet). | 10% donkey serum (Sigma) in PB blocking solution** | Donkey anti-goat (1:500, Alexa fluor 488, Life Technologies) |
| NeuN<br>Brightfield<br><br>Mouse Monoclonal (Millipore)<br><br>1:5,000 | Raised against purified cell nuclei from mouse brain. Specificity in mature neurons has been demonstrated (Mullen et al., 1992) | 5% horse serum (Vector) in Tris blocking solution* | Horse anti-mouse (1:400, Vector) |
| Ki67<br>Confocal<br><br>Rabbit Polyclonal (Vector)<br><br>1:500 | Raised against a recombinant fusion protein corresponding to a 1086bp cDNA fragment containing the Ki67 motif. Specificity has been demonstrated (Gerdes et al., 1991; Key et al., 1993; Schluter et al., 1993) | 10% donkey serum (Sigma) in PB blocking solution** | Donkey anti-rabbit (1:500, Alexa Fluor 546, Life Technologies) |
| Doublecortin<br>Confocal<br><br>Goat Polyclonal (Santa Cruz Biotechnology)<br><br>1:500 | Raised against the C-terminus of human DCX. Specificity for immature neurons has been demonstrated (von Bohlen Und Halbach, 2007) | 10% donkey serum (Sigma) in PB blocking solution** | Donkey anti-goat (1:500, Alexa Fluor 568, Life Technologies) |

**Legend:**

Information supporting the specificity of antibodies and their preparation is listed. * Tris blocking solution = 0.25% Triton X-100 and 0.005% bovine serum albumin in 0.1 M Tris buffer. ** PB blocking solution = 0.25% Triton X-100 and 0.005% bovine serum albumin in 0.1 M PB.

**Supplemental Figure 1. Hilar Prox1-ir cell population size and hilar volume of C57BL6/J mice at PND 16, 30, and 60.**

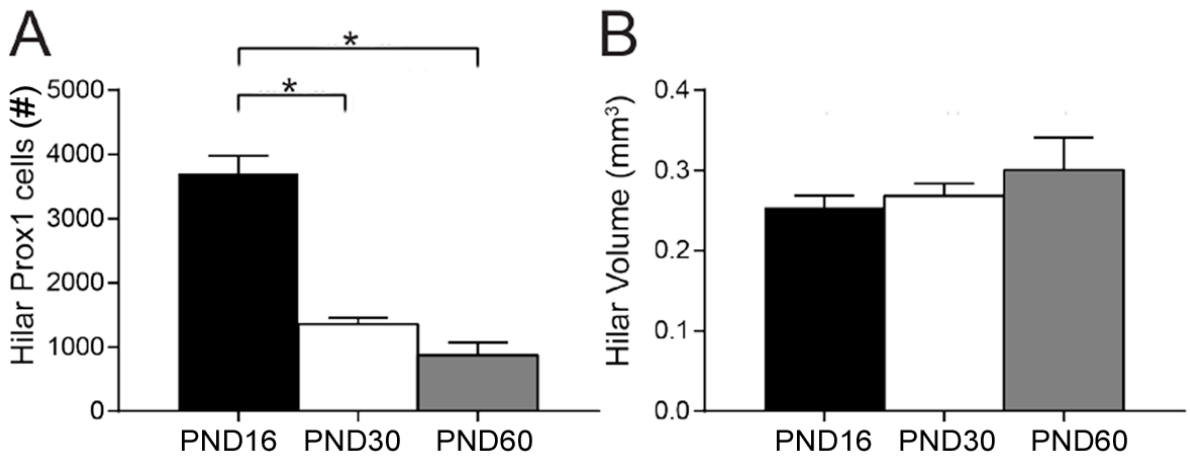


**Legend:**

A. Cell numbers are shown for C57BL6/J mice at three ages (PND16, n=4; PND30, n=5; PND60, n=5). All groups were significantly different by one-way ANOVA ($F(2,11)96.38$; $p < 0.0001$) and post-hoc tests showed that PND16 cell numbers were greater than either PND30 or PND60 ($p < 0.05$; asterisks).

B. Hilar volume at three ages. There were no significant differences ($F(2,11)2.86$; $p=0.0997$).

**Supplemental Figure 2. Detailed images of Prox1-calretinin double-labeling shown in Figure 3.**

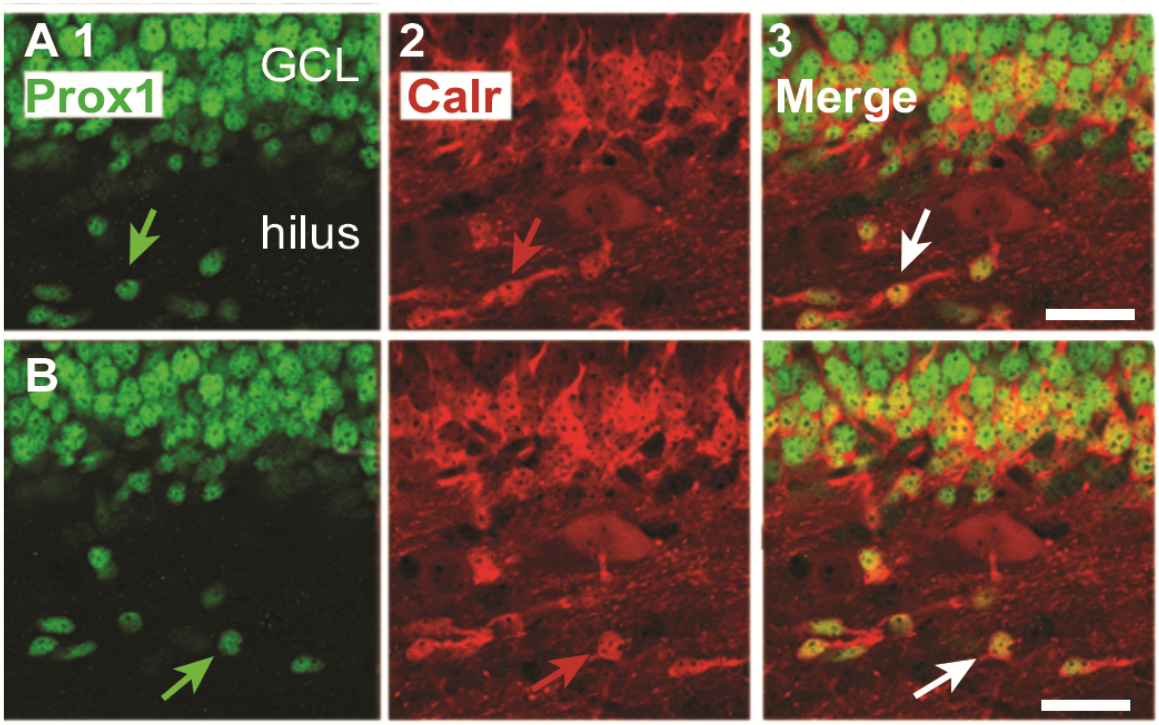


**Legend:**

A. 1. A section from a PND16 C57BL6/J mouse stained for Prox1(green) shows numerous Prox1-ir cells in the GCL and some in the hilus (green arrow).

2. The same section showing calretinin-immunorfluorescence (Calr, red) shows many cells at the GCL/hilar border and some in the hilus, including the cell that was stained with Prox1 (red arrow).

3. A merged image shows double-labeled cells (yellow) at the GCL/hilar border and in the hilus (arrow).

B. A different optical section of the same tissue in A illustrates that cells which were not clearly double-labeled in one optical section (in A) were often double-labeled in the adjacent optical section (in B). An example is identified by the arrows.

**Supplemental Figure 3. Detailed images of Prox1-DCX double-labeling shown in Figure 3.**

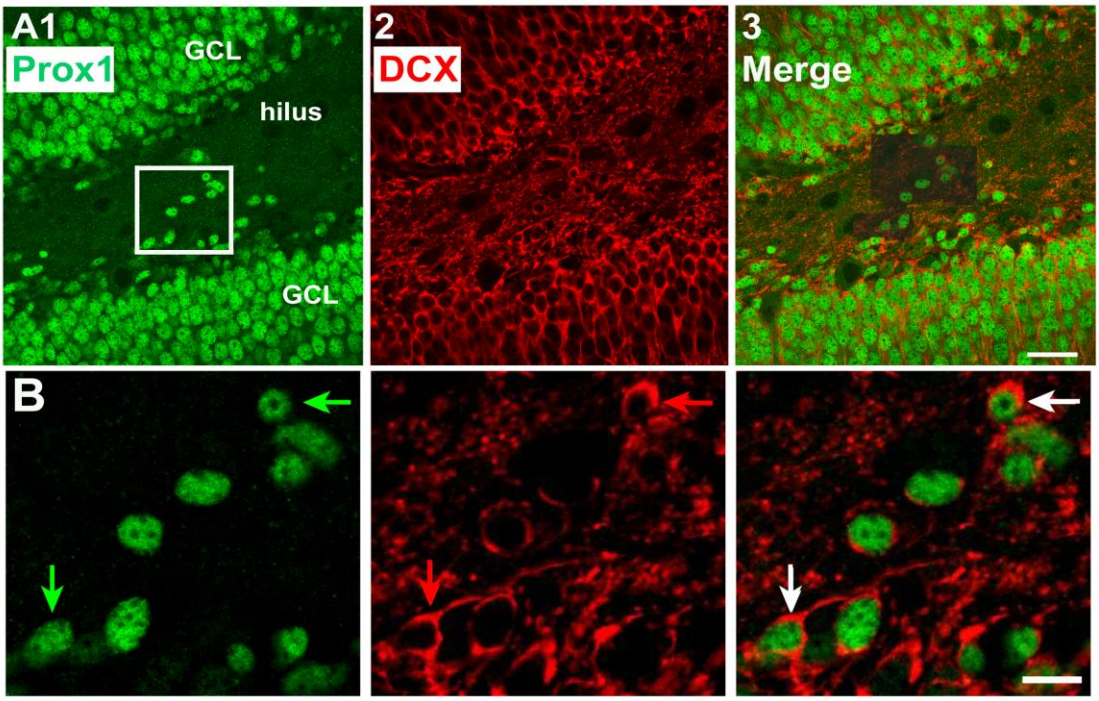


**Legend:**

A. A tissue section from a C57BL6/J mouse stained for Prox1 (green, 1) and DCX (red, 2). The merged image is shown in 3. The area outlined by the box in A1 is expanded in B. Calibration, 25 µm.

B. Prox1-immunofluorescent cells (green arrows, 1) were often labeled by DCX (red arrows, 2) with the merged image (3) showing a green nucleus outlined by red cytoplasm (white arrows). Calibration, 10 µm.

**Supplemental Figure 4. Comparisons of hilar Prox1-ir cells in septal and temporal sections of C57BL6/J mice.**

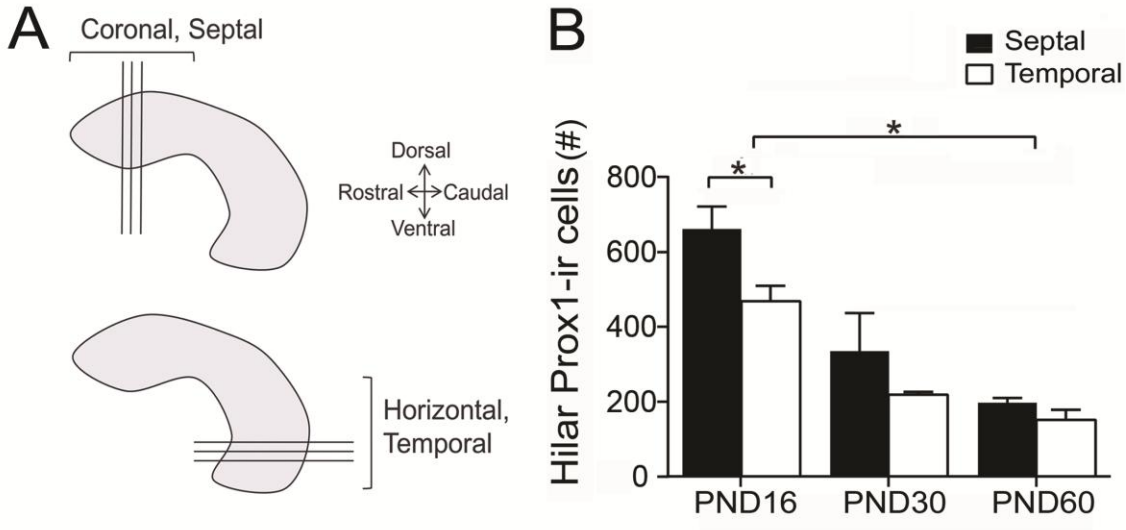


**Legend:**

A. A schematic shows the procedure to make coronal sections from septal hippocampus and horizontal sections of temporal hippocampus. The brackets indicate the approximate span where sections were selected.

B. Mean values for hilar Prox1-ir cell density in sections cut either in the coronal or horizontal plane. Four-5 sections were selected from septal DG cut in the coronal plane and 4-5 sections were selected from temporal DG cut in the horizontal plane (see Methods). Two-way ANOVA showed a significant effect of septotemporal location ($F(1,12)$ 23.26; $p = 0.0004$ ) with greater cell density in septal DG relative to temporal DG at PND16 (post-hoc tests, $p < 0.05$, asterisks) but not other ages ($p > 0.05$). ns = not significant.

**Supplemental Figure 5. Hilar Prox1-ir cell population size and hilar area along the septotemporal axis.**

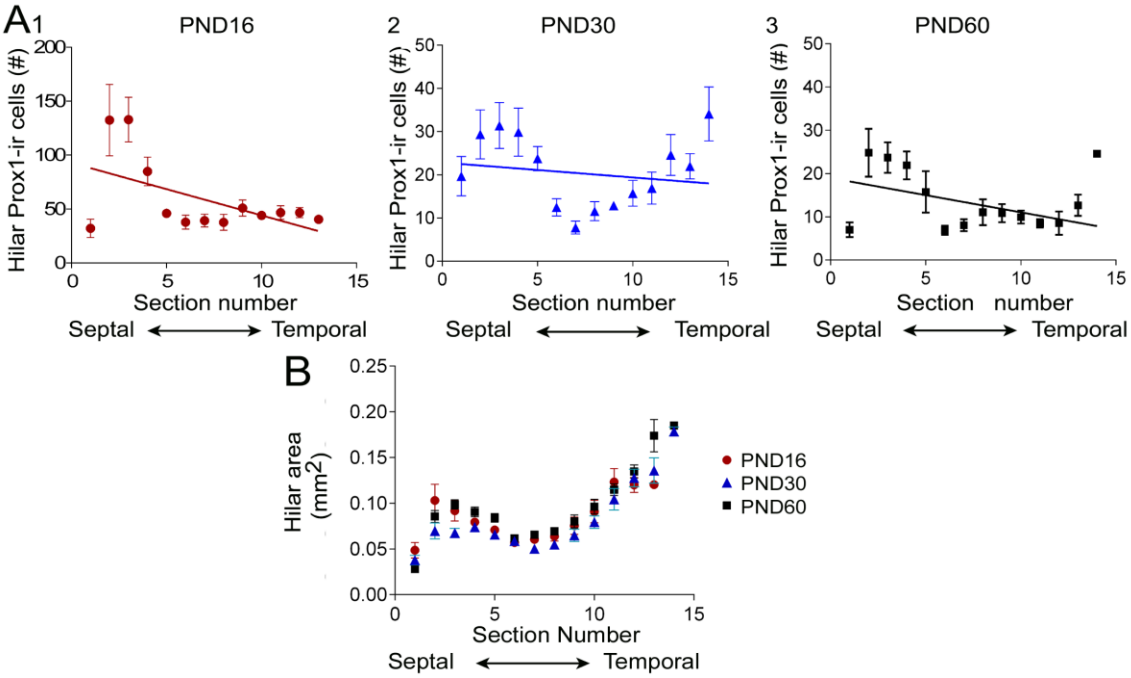


**Legend:**

A. Hilar Prox1-ir cells were most numerous in the septal sections of isolated hippocampi in C57BL6/J mice. 1) PND16; 2) PND30; 3) PND60. Same sample sizes as Figure 1D.

B. Hilar area varied along the septotemporal axis in a similar manner for all three postnatal ages. Same sample sizes as Figure 1D.

**Supplemental Figure 6. Hilar Prox1-ir cell population size and hilar volume in Nestin-Cre Bax$^{f/f}$ mice.**

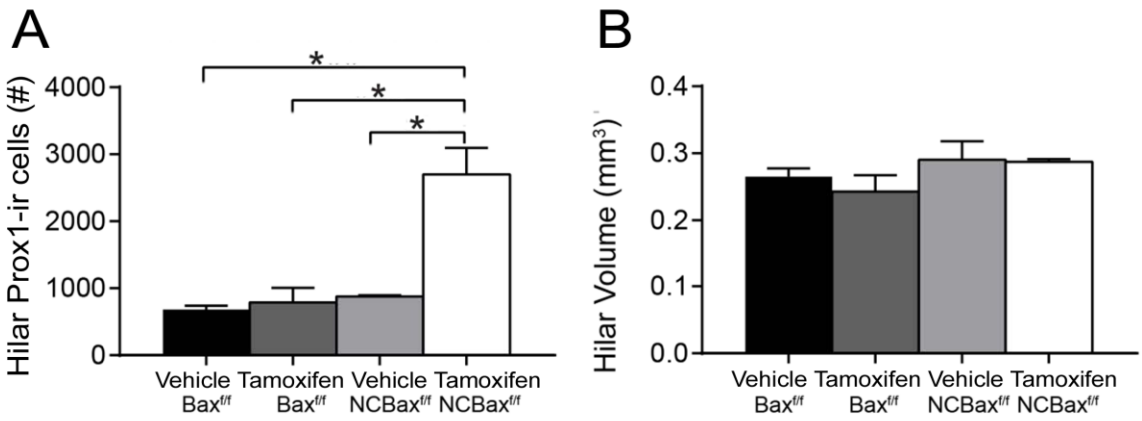


**Legend:**

A. Hilar Prox1-ir cell population size for isolated hippocampi from transgenic mice (n=3/group). The four groups were: tamoxifen- or vehicle- treated NCBax$^{f/f}$ and tamoxifen- or vehicle-treated Bax$^{f/f}$ mice. One-way ANOVA showed that the groups were significantly different ($F(3,8)$ 20.88; $p = 0.0004$), with the tamoxifen-treated NCBax$^{f/f}$ mice greater that all other groups (post-hoc test, $p < 0.05$; asterisks).

B. Hilar volumes in the four groups were not significantly different ($F(3,8)3.065$ ; $p = 0.0912$).

**Supplemental Figure 7. NCBax$^{f/f}$ mice at PND30 and PND60 days showed similar results.**

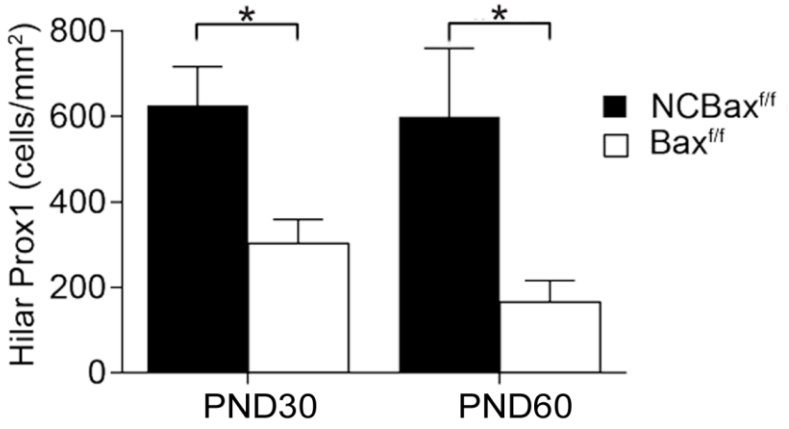


**Legend:**

Hilar Prox1-ir cells are shown for PND30 and PND60 mice. For this comparison, sections were collected from hemispheres of 3 mice (PND30) or 4 mice (PND60) and the sections from the center of the septal hippocampus were used (4-5 sections/mouse). NCBax$^{f/f}$ mice were tamoxifen-treated and Bax$^{f/f}$ mice were also tamoxifen-treated. A two-way ANOVA showed a main effect of genotype ($F(1,10)45.13$; $p < 0.0001$) but not age ($F(1,10)2.140$ ; $p = 0.1742$). PND30 NCBax$^{f/f}$ mice had a greater cell density than Bax$^{f/f}$ mice (post-hoc test, $p < 0.05$) and the same was true for PND60 ($p < 0.05$).

**Supplemental Movie 1.**

Prox1/calretinin double-immunofluorescence is shown for a z-stack from a C57BL6/J mouse. The granule cell layer is well labeled and at lower right. It is visible in most of the z-stack. The hilar cells in the center are rare and only visible in some of the z-stack. Note that the Prox1 (green) and calretinin (red) labeling comes into focus in the same optical sections, suggesting that double labeling has occurred.

## References


Gerdes J, Li L, Schlueter C, Duchrow M, Wohlenberg C, Gerlach C, Stahmer I, Kloth S, Brandt E, Flad HD (1991) Immunobiochemical and molecular biologic characterization of the cell proliferation-associated nuclear antigen that is defined by monoclonal antibody Ki-67. Am J Pathol 138:867-873.

Key G, Becker MH, Baron B, Duchrow M, Schluter C, Flad HD, Gerdes J (1993) New Ki-67-equivalent murine monoclonal antibodies (MIB 1-3) generated against bacterially expressed parts of the Ki-67 cDNA containing three 62 base pair repetitive elements encoding for the Ki-67 epitope. Lab Invest 68:629-636.

Lavado A, Lagutin OV, Chow LM, Baker SJ, Oliver G (2010) Prox1 is required for granule cell maturation and intermediate progenitor maintenance during brain neurogenesis. PLoS Biol 8.

Mullen RJ, Buck CR, Smith AM (1992) NeuN, a neuronal specific nuclear protein in vertebrates. Development 116:201-211.

Ridler TW, Calvard S (1978) Picture Thresholding Using an Iterative Selection Method. Systems, Man and Cybernetics, IEEE Transactions on 8:630-632.

Schluter C, Duchrow M, Wohlenberg C, Becker MH, Key G, Flad HD, Gerdes J (1993) The cell proliferation-associated antigen of antibody Ki-67: a very large, ubiquitous nuclear protein with numerous repeated elements, representing a new kind of cell cycle-maintaining proteins. J Cell Biol 123:513-522.

von Bohlen Und Halbach O (2007) Immunohistological markers for staging neurogenesis in adult hippocampus. Cell Tissue Res 329:409-420.